MINISTRY OF AVIATION

AERONAUTICAL RESEARCH COUNCIL
REPORTS AND MEMORANDA

Measurement of the Performance of a Single Stage, High Mach Number, Subsonic Axial-Flow Compressor

By R. STANIFORTH

Measurement of the Performance of a Single Stage, High Mach Number, Subsonic Axial-Flow Compressor

By R. Staniforth

Communicated by the Director General of Scientific Research (Air),
Ministry of Supply

Summary. A subsonic compressor designed to operate at high Mach numbers was tested, the measured pressure ratio being 1·38 at 22 lb/sec/sq ft flow and about 89 per cent efficiency. This efficiency was maintained at 5 per cent overspeed, but at still higher speeds the efficiency fell noticeably.

The measured performance differed from the design figures because of secondary flows which caused large radial gradients in temperature rise and pressure ratio.

The presence of both radial temperature and pressure gradients together with secondary flows made the accurate determination of the compressor efficiency difficult—the method normally used giving an efficiency about 3 per cent lower than a more accurate method using results taken during traversing after the stator. Whilst the low aspect ratio and non-uniform work addition of the present compressor accentuate these difficulties, they must exist to some extent in all single stage tests. To overcome this snag, it would seem desirable to install additional instrumentation for overall efficiency measurement some way downstream from the compressor stator row, where the flow is more uniform.

1.0. *Introduction.* In continuance of an investigation into the characteristics of high duty axial-flow compressors, a compressor was constructed and tested which was designed to operate at the highest Mach numbers considered permissible according to the then accepted rules. The tests were intended for comparison with those of the previously tested transonic design[1] and also to yield information on the behaviour of the blade section C.3, which was used.

2.0. *Description of Compressor.* As the design details have not previously been recorded, a description of some of the more important features is included in this Report.

2.1. *Design.* Obviously, all details of compressor design cannot be determined by simple rational argument; many depend on the designer's experience, and others are just generally accepted practice. Into these categories fall the use of the following features:

(1) Fifty per cent reaction at mean diameter.
(2) Radially constant work input.
(3) Radially constant axial velocity and constant axial velocity through the compressor.
(4) Design tip speed = 1,080 ft/sec.
(5) Blade thickness/blade chord at rotor tip = 4 per cent.
(6) Rotor blade chord reduced 10 per cent from root to tip.
(7) The aspect ratio of the blade rows should be greater than 1.

The design rules for determining the nominal or design deflection, and the nominal deviations, were those of References 2 and 3 respectively and, finally, the physical design of the test rig limited the compressor diameter ratio to about 0·62 at the rotor inlet.

In a high speed compressor, the important limitations on pressure ratio and flow are tip and root critical Mach number and the blade stress at the hub. The stress and aerodynamic behaviour at the hub are interdependent because the thickness of the blade also affects the critical Mach number. Throughout this design, the maximum root stress was governed by an overspeed condition of 23,000 r.p.m. at which the specified ratio of the maximum permissible alternating stress (from a Goodman diagram) to the maximum stress due to air load, *i.e.*, the fatigue factor, was 3.

To simplify the analysis, the method of predicting the critical Mach number of a cascade of blades described in Reference 4 was used in a slightly modified form. This modification involved the substitution of the inlet Mach number for the outlet Mach number in the formula and the making of appropriate changes in the constants. This step is quite justifiable because the ratio inlet Mach number/outlet Mach number is fairly constant in this design on account of its large diameter ratio.

The critical Mach number of a cascade of blades is then given by

$$0·96 \left[1 - \frac{t/c}{0·45\, s/c} \right]$$

the constant, 0·96, being determined from earlier tests on a high duty compressor.

Four common types of compressor blade twist were considered: free vortex, constant α_4, constant α_3 and constant reaction. It was shown that in this particular case, constant α_3 blading gave the highest stage temperature rise, and this feature was therefore adopted in the design.

It should be noted that the assumption of a radially constant Va, temperature rise and α_3 implies a radially constant Mach number into the stator, and the specification of 50 per cent reaction at mean diameter makes this equal to the Mach number into the rotor at mean diameter. As the stators are subject to lower stresses than the rotor (due to the absence of centrifugal loads) they can be made thinner than the rotor blades to give a higher critical Mach number if required. Thus the choice of a constant α_3 design involves no stator design problem.

An investigation into the effect of mean diameter α_2 and s/c on the specific flow and temperature rise of a compressor stage indicated that a fair compromise could be reached using a mean diameter α_2 of about 25 deg (in the final design, taken to be 25·6 deg) and a mean diameter s/c of 0·9.

In the analysis summarised above, it was assumed that the rotor blades would be made of a magnesium alloy. The reason for this choice was that steel blades in this particular rig would have introduced high disc stresses under overspeed conditions without allowing the work capacity to be appreciably increased.

The final design figures for the stage were taken as a temperature rise of 30 deg C and an inlet axial velocity of 550 ft/sec, which with the previously mentioned limitation in diameter ratio to 0·62, gives a specific flow of 22·0 lb/sec/sq ft.

2.2. *Velocity Triangles.* Having decided that the blade twist should be such as to give constant α_3 with $\alpha_2 = 25·6$ deg at the mean diameter and a temperature rise of 30 deg C, the remaining air angles and other details can be readily calculated (Figure 1). The blade angles were then determined using References 2 and 3, a summary of the results being given in Appendix I.

2.3. *Blade Section.* The blade sections used in this compressor obviously had to have a good high speed performance. Both cascade and compressor tests have shown that profiles having their

maximum thickness at about 50 per cent chord are superior to the more usual types where the maximum thickness is at 30 per cent chord from the leading edge, so that the obvious choice was either a two-arc blade or one using the C.3 (Reference 5) blade section. Many compressors have now been tested which used the former shape, whereas apart from cascade tests, little is known about the performance of the C.3 section. Mainly for this reason, the C.3 section was used throughout this compressor.

Cascade tests on C.3 profile cascades have been conflicting; early tests[5] suggested only that they had a reduced incidence range compared with the range of a normal aerofoil cascade, whereas later tests[6,7,8] suggested that this range was very small. This inconsistency is now established as due to low Reynolds numbers in the second series of tests allowing a laminar boundary layer to persist along the convex surface (at negative incidence) to a steep pressure gradient at about 50 per cent chord where it then separates. The reason for the persistence of the laminar flow can be more readily appreciated from a study of the pressure distribution over C.3 blades in cascade[9]. However, as large blade chords were specified for these tests, and the expected turbulence was quite high, it was considered unlikely that this trouble would be experienced in the compressor.

3.0. *Experimental Installation and Instrumentation.* Tests in the rig on a transonic compressor[1] showed that the circuit loss was too high to permit this subsonic design to run unstalled, and therefore some air circuit modifications were essential. At the same time it was considered advantageous to replace the multi-hole orifice-plate flow meter with a calibrated nozzle in the compressor inlet as this would simplify corrected flow measurement. This change would also reduce the circuit loss considerably, but as an additional precaution and also for inlet guide vane tests, an ejector was installed in the compressor outlet immediately following the throttle. This ejector was not required for the present tests because of the fairly high pressure ratio developed by the compressor.

3.1. *Intake and Flow Measuring Nozzle.* With the above modifications, the test rig air circuit was as sketched in Figure 2. Air is drawn by the compressor from a spacious building adjacent to the test cubicle through a honeycomb, a contraction and then a diffuser to the original 3 ft intake duct containing a further honeycomb and two gauzes. After the compressor, the air passes through a throttle and then through the ejector, which replaces the settling length of the earlier orifice plate, into the silencer.

Calibration tests on the measuring nozzle were made by sucking air through the rig with a dummy compressor installed, the nozzle being traversed at four circumferential stations to determine the flow coefficient, *i.e.*, the ratio of the actual flow as found by traversing to that indicated from a central pitot and wall statics. The coefficient thus determined was 0·990.

3.2. *Compressor Stage.* The arrangement of the compressor stage in the rig, showing the approximate positions of the measuring instruments, is given in Figure 3. Two circumferential traverse instrument rings were fitted, one to permit traversing between the inlet guide vane and rotor and the other for traversing downstream of the outlet stator.

The instrumentation layout was substantially the same as that described in Reference 1, the only change being an allowance for the different number of blades and annulus height in the two builds. There were two additions; statics were fitted between the blade rows (one in the inner wall and two or three in the outer wall at each station) and provision was made for the more accurate measurement of the mean diameter temperature rise using a network of four thermo-couples in series, two in the inlet duct and two downstream of the stator.

3

4.0. *Experimental Procedure.* This was almost identical to that of Reference 1, readings being taken at corrected speeds of 14,000, 16,000, 18,000, 19,000, 20,000, 21,000, 22,000, 23,000 and 24,000 r.p.m. for throttle settings from full open to the surge point. To avoid confusion, only the results at 14,000, 18,000, 21,000, 22,000, 23,000 and 24,000 r.p.m. are actually given in this Report, the last three being overspeed.

After a first test series carried out as above, some detailed traverses were made after the stators. As the range of circumferential travel was only just equal to one blade pitch, it was necessary to move the stator blades peripherally to bring their wake into the middle of this range. Following these traverses, a new test series similar to the first was completed as a check on the earlier readings.

The above-mentioned traverses after the stator were made at a few selected throttle settings at a number of speeds and consisted of readings of pressure and temperature from the radial pressure and temperature combs at several stations over a whole stator blade pitch. In addition, circumferential traverses were made with a remotely operated pitot yawmeter between the inlet guide vanes and rotor to determine the inlet guide-vane air exit angles. This was done at a fixed speed of 15,000 r.p.m. and a throttle setting approximating to the maximum efficiency point on the characteristic.

The surge of the compressor in this particular test configuration was quite gentle: at low speeds, at about 10,000 r.p.m., some hysteresis was present, but none could be detected near the design speed, at 21,000 r.p.m.

5.0. *Results.* 5.1. *Overall Performance.* The experimental readings were reduced to give the compressor efficiency, pressure ratio and mass flow as described in Appendix II. In Section 4.0 it was mentioned that two sets of readings were taken, the second after an adjustment had been made to the circumferential position of the stator. Whilst each set of results was in itself consistent, it was immediately apparent that there were discrepancies between the sets which were too large to be accounted for by instrumentation or reading errors. This effect, it was concluded, was due to the change of position of the instrumentation relative to the inlet guide vane—the downstream instrumentation following the adjustment made to the stator position. The mean pressure ratios and efficiencies, *i.e.,* mean curves drawn through all the points taken in both test series, are shown in Figure 4.

5.2. *Inlet Guide Vane Traverse.* These test results revealed that the blades were operating properly; skin-friction loss was low and there was no evidence of flow separation. This was confirmed by later tests in which air was drawn over the inlet guide vanes with an ejector, by observing tufts attached to the blade surface. However, there was a considerable discrepancy between the design and the experimental air angles (Figure 5), the reason for this being discussed later in Section 6.0.

5.3. *Performance Derived from Traverses Downstream of Stators.* From the more detailed information supplied by the traverses downstream of the stator, the compressor efficiency could be determined with greater precision. The method used was to calculate area means of both temperature and pressure rise by integrating, first circumferentially and then radially over one blade pitch (Appendix III). As a check that these data were consistent with those used earlier to determine the overall performance (Section 5.1), the necessary information was selected from the traverse data taken at 21,000 r.p.m. and the performance recalculated as in Appendix II. The performance data determined from the traverse readings are plotted in Figure 6.

4

6.0. *Discussion.* Referring to the compressor characteristics of Figure 4, it will be noticed that the recorded efficiency drops gradually from 92 per cent at 14,000 r.p.m. to 86 per cent at 22,000 r.p.m. —about 5 per cent above design speed—but that at higher speeds the peak efficiency is considerably lower. This drop in performance being due to high speed stalling of the compressor blades, it appears that the critical Mach numbers assumed in design were a little pessimistic. As the Mach number in the rotor is a little higher than that in the stator, it might be expected that the rotor would shock stall first. This view is supported by velocity profiles after the stator which show little increase in the profile loss between 22,000 and 24,000 r.p.m.

The flow range for efficient operation at low speed is substantially smaller than that expected from an equivalent stage using C.4 aerofoils. This is shown clearly in Figure 7 which compares the measured performance of the compressor with the estimated performance of an equivalent C.4 stage[10] (using the design air angles, work done factor of one, and neglecting Mach number effects). At 21,000 r.p.m. the surge point is at a lower incidence than at 14,000 r.p.m. thus showing the usual reduction in positive stalling incidence with increasing Mach number. The choking flow at 21,000 r.p.m. agrees satisfactorily with the value estimated from the measured throat area of the rotor (the rotor choking before the stator).

The discrepancy between the calculated or design, and the measured pressure ratio, must be connected with secondary flow effects, for it is unlikely that, with approximately two dimensional flow, errors in the estimated deviation could alone cause the observed difference. Because the rotor, stator and inlet guide blades all have similar aspect ratios and lengthwise circulation variations, it is reasonable to expect that roughly similar discrepancies in the air leaving angle must exist in all three blade rows. Both the inlet guide vane and rotor secondary effects might thus be expected, on an average, to increase the work done by the stage whilst causing the temperature rise and pressure ratio at the outside to be considerably greater than at the inner diameter. The latter is confirmed directly by the traverse results in Figure 8. Although, as is common practice, the effects of secondary flows were neglected in the design, the measured flow differences were not entirely unexpected and, in fact, they could have been predicted using available analytical techniques.

From the traverse results taken behind the stator, two things were established: the radial variation in performance, and a more precise measure of the efficiency and pressure ratio. Because of the large radial gradient in temperature rise, plus the secondary flow, the variation in total temperature and pressure from point to point in the annulus is large and, consequently, any determination of the detailed rotor blade performance must be of dubious accuracy. For this reason it was not possible to decide which section stalled first when surge was approached, or whether it was the rotor root or the tip which shock stalled first.

The overall pressure ratios and efficiencies calculated from the traverse results did, however, shed considerable light on the reliability of the methods generally used. But it should be remembered that the figures quoted here are for a compressor of low aspect ratio which, through its generation of large secondary flows and consequent effect on the radial distribution of work makes the accurate determination of the characteristics more difficult than in the average case. Figure 6, which compares the efficiencies and pressure ratios obtained by traversing with those determined from fixed instrumentation indicates that the true efficiency does not really fall as much with increasing speed as thought previously and that the simpler instrumentation underestimates the maximum efficiency by at least 3 per cent at 21,000 r.p.m. In addition, the traverse tests tend to indicate that the efficiency

5

·does not drop off as surge is approached and they suggest figures which agree more favourably with the calculated values of Figure 7.

As the three test points calculated as Appendix II from data selected from the traverse results confirmed the earlier characteristics, there can be no doubt that the above discrepancies were simply due to the fact that the data from the fixed instrumentation were not truly representative.

It will be remembered that the mean temperature rise is determined on an area basis, whereas strictly a mass basis should have been used. The determination of the mass mean would necessitate the taking of many more readings and would complicate the subsequent analysis. However, by taking a second set of readings in the more uniform air stream some way downstream from the stator, where the flow will be more uniform, a valuable accurate check on the overall compressor performance could be obtained without excessive computation.

7.0. *Conclusions.*   The compressor gave a pressure ratio of $1 \cdot 38$ at 22 lb/sec/sq ft mass flow at about 89 per cent efficiency, the latter being maintained at 5 per cent overspeed where the Mach number of the air relative to the rotor tip was $0 \cdot 94$ and to the mean diameter $0 \cdot 8$. At higher speeds, the efficiency fell noticeably.

Because of the low aspect ratios used in the compressor, secondary flows were important in that they caused radial gradients in temperature rise across the annulus. This resulted in large variations in pressure and temperature at the measuring plane downstream of the stator, which effect made the measuring of the overall pressure ratio and efficiency difficult.

Two methods of determining the performance were employed, the first using only two sets of fixed instrument combs—instruments disposed radially at the middle of the stator blade passage and circumferentially at mid-blade height. In the second, the radial combs (both pressure and temperature) were traversed across one blade passage, with the result that the efficiency and pressure ratio thus recorded were higher than with the first method.

It is suggested that in any further tests a separate set of instruments be installed some way downstream of the compressor stator, where the flow will be more uniform than that in the stator exit plane, so that an accurate and independent check can be made on the overall compressor performance.

The blade section used, namely C.3, performed well at high Mach numbers and in that a high efficiency was measured, the selected design rules appeared satisfactory. However, the installed incidence range at moderate speeds was a little less than for an equivalent C.4 section, which fact caused the surge and design points to be closer together than is usual.

LIST OF SYMBOLS

c	Blade chord
M	Mach number
s	Pitch of blades
t	Blade thickness
V	Velocity (ft/sec)
α	Direction of air flow relative to axial direction

Suffices (applied to M, V and α)

0	Absolute at inlet guide vane outlet
1	Relative to rotor at rotor inlet
2	Relative to rotor at rotor outlet
3	Absolute at stator inlet
4	Absolute at stator outlet
a	Axial component

REFERENCES

No.	Author(s)	Title, etc.
1	R. Parker	Measurement of the performance of a single stage transonic axial flow compressor. A.R.C. 19,796. October, 1957.
2	A. D. S. Carter and A. F. Hounsell	General performance data for aerofoils having C.1, C.2 or C.4 base profiles on circular arc camber lines. A.R.C. 12,889. August, 1949.
3	A. D. S. Carter	The low speed performance of related aerofoils in cascade. A.R.C. C.P. 29. September, 1949.
4	A. D. S. Carter and Hazel P. Hughes	A note on the high speed performance of compressor cascades. A.R.C. 12,708. December, 1948.
5	A. R. Howell	A note on compressor base aerofoils C.1, C.2, C.3, C.4, C.5 and aerofoils made up of circular arcs. Power Jets Memorandum No. M.1011. September, 1944.
6	Staff of Aerodynamics Department	A test on a compressor cascade of aerofoils having their position of maximum thickness 50 per cent of the chord from the leading edge. A.R.C. 12,658. August, 1949.
7	G. K. Korbacher and A. Smith	A test on a compressor cascade of aerofoils having their position of maximum thickness 50 per cent of the chord from the leading edge at a pitch/chord ratio of 0·75. A.R.C. 19,093. December, 1949.
8	G. K. Korbacher	A test on a compressor cascade of aerofoils having their position of maximum thickness 50 per cent of the chord from the leading edge and a pitch/chord ratio of 1·25. A.R.C. 13,673. May, 1950.
9	A. D. S. Carter and Hazel P. Hughes	A theoretical investigation into the effect of profile shape on the performance of aerofoils in cascade. A.R.C. R. & M. 2384. March, 1946.
10	A. R. Howell	Fluid dynamics of axial compressors. I.Mech.E. Proc. Vol. 153 (WEP. No. 12). 1945.

APPENDIX I

Compressor details

Annulus dimensions

Constant outer diameter	12 in.
Constant inner diameter through inlet guide vanes	7·5 in.
Inside diameter after rotor	8·15 in.
Outside diameter after stator	8·56 in.
Axial spacing between blade centre-lines	2·30 in.

Blade data

Inlet guide vanes 18 blades in aluminium alloy

Diameter (inches)	7·9	9·75	11·6
Camber (degrees)	21·7	31·3	37·7
Stagger (degrees)	+10·85	+15·65	+18·85
Chord (inches)	1·81	1·89	1·97
Thickness/chord	0·052	0·060	0·068

Rotor 19 blades in magnesium alloy

Diameter (inches)	8·4	9·75	11·6
Camber (degrees)	42·6	34·4	26·0
Stagger (degrees)	−26·5	−33·8	−42·7
Chord (inches)	1·852	1·795	1·720
Thickness/chord	0·067	0·056	0·043

Stator 20 blades in aluminium alloy

Diameter (inches)	8·90	9·75	11·6
Camber (degrees)	37·7	34·4	29·2
Stagger (degrees)	−32·2	−33·8	−36·4
Chord (inches)	1·67	1·70	1·77
Thickness/chord	0·056	0·060	0·068

Stressing

Aerodynamic design speed	20,640 r.p.m.
Mechanical design speed with a fatigue factor of 3	23,000 r.p.m.

APPENDIX II

Reduction of Fixed Instrument Data

The effective total pressure at the outlet of the compressor was calculated from data from two sets of instruments mounted just downstream of the stator; a radial pitot comb and a circumferential one. These combs, together with the temperature probes mentioned later, were mounted on a ring which could be turned in a peripheral direction until the centre tube of the circumferential comb was in the centre of the stator blade wake. This adjustment placed the radial pitot comb and the individual temperature probes midway between the stator wakes. From the various comb readings, the compressor pressure ratio and efficiency were calculated as follows.

Pressure Ratio. The readings from the circumferential comb were plotted against distance and a mean value determined with the use of a planimeter. The ratio of this mean pressure to the mean of the pressures indicated by the end tubes of the comb, termed the recovery factor, was then calculated.

An area mean of the radial comb readings was next determined simply by weighting each reading with radius, for an area mean was desired, and then adding up the resulting figures by means of the following formula:

Mean pressure =

$$\frac{2}{\left(\text{No. of tubes in comb}\right)\left(1 + \dfrac{\text{inner radius}}{\text{outer radius}}\right)} \Sigma \text{ Pitot reading} \times \frac{\text{radius}}{\text{outer radius}}.$$

Then, on the assumption that the recovery factor determined at the mean diameter was representative of the stator as a whole, the mean pressure at the stage outlet is the product of this factor and the mean pressure from the radial comb readings. The stage pressure ratio can then be determined, as the inlet pressure to the stage is that recorded in the 3 ft duct leading to the compressor.

Temperature Rise. The total temperatures across the annulus downstream of the stator were measured with five separate probes at different peripheral stations. Because the mean height readings were suspect, the readings from the network of four probes at mean diameter were substituted in the analysis. Most of the reduction of data was carried out before conversion of the thermo-electric voltage into an actual rise in temperature, for the temperature-millivolts from the thermo-junction relationship was practically linear in the temperature range involved.

As with the radial pressure comb data, so with the temperature probe data the mean temperature rise was determined by addition by means of the following formula:

Mean temperature rise (millivolts) =

$$\frac{2}{\left(\text{No. of probes in comb}\right)\left(1 + \dfrac{\text{inner radius}}{\text{outer radius}}\right)} \times \Sigma \text{ Probe millivolts} \times \frac{\text{radius}}{\text{outer radius}}.$$

The resulting figure was then converted into a temperature rise using an accurate calibration curve.

Efficiency. Given the pressure ratio and the actual temperature rise, all that is required is the isentropic temperature rise at the given pressure ratio and inlet temperature, and then the efficiency, being equal to the isentropic temperature rise divided by the actual temperature rise, can be calculated. It should be noted that the efficiency calculated as just described is for the complete stage and includes the effect of inlet guide vane loss. Because the rig was tested at particular corrected speeds and the airflow was derived directly as a corrected flow, no correction was necessary to account for non-standard inlet conditions.

APPENDIX III

Reduction of the Traverse Data

The data were reduced in a very similar manner to that described in Appendix II except that they were first integrated circumferentially over one blade pitch to determine the average circumferential reading for each radial station before integrating radially.
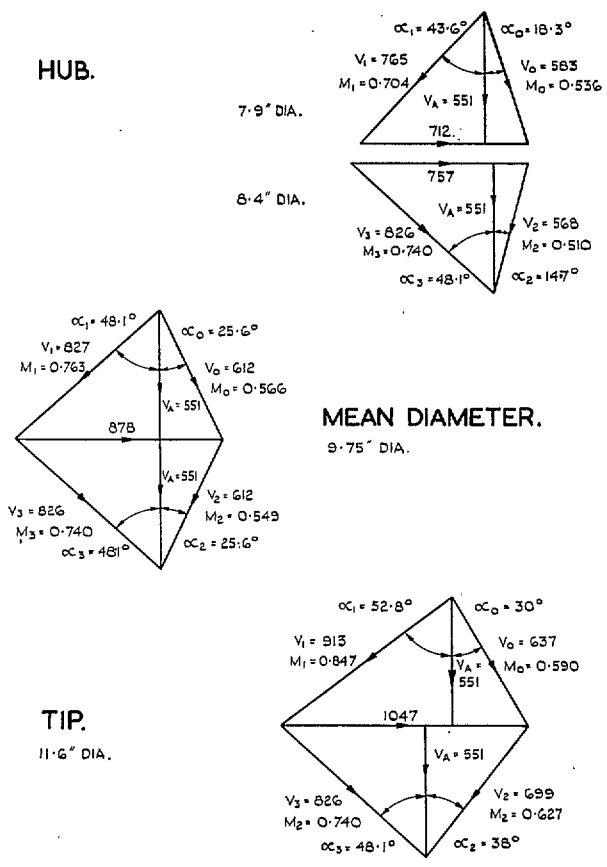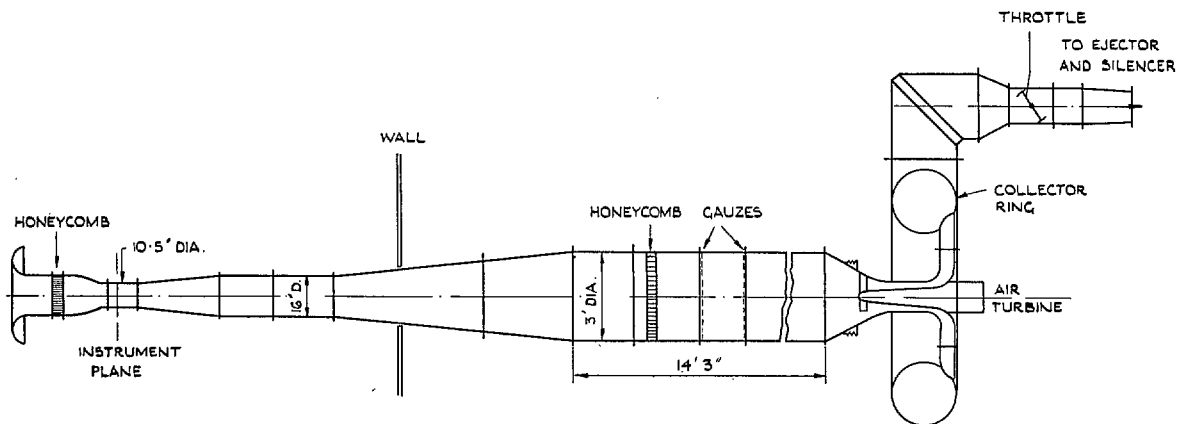
HUB.

7·9" DIA.

8·4" DIA.

$\alpha_1 = 43\cdot6°$ $\alpha_0 = 18\cdot3°$
$V_1 = 765$ $V_0 = 583$
$M_1 = 0\cdot704$ $M_0 = 0\cdot536$
$V_A = 551$
712.

757
$V_A = 551$
$V_3 = 826$ $V_2 = 568$
$M_3 = 0\cdot740$ $M_2 = 0\cdot510$
$\alpha_3 = 48\cdot1°$ $\alpha_2 = 14\cdot7°$

$\alpha_1 = 48\cdot1°$ $\alpha_0 = 25\cdot6°$
$V_1 = 827$ $V_0 = 612$
$M_1 = 0\cdot763$ $M_0 = 0\cdot566$
$V_A = 551$

MEAN DIAMETER.
9·75" DIA.

878
$V_A = 551$
$V_3 = 826$ $V_2 = 612$
$M_3 = 0\cdot740$ $M_2 = 0\cdot549$
$\alpha_3 = 48\cdot1°$ $\alpha_2 = 25\cdot6°$

$\alpha_1 = 52\cdot8°$ $\alpha_0 = 30°$
$V_1 = 913$ $V_0 = 637$
$M_1 = 0\cdot847$ $M_0 = 0\cdot590$
$V_A = 551$

TIP.
11·6" DIA.

1047
$V_A = 551$
$V_3 = 826$ $V_2 = 699$
$M_3 = 0\cdot740$ $M_2 = 0\cdot627$
$\alpha_3 = 48\cdot1°$ $\alpha_2 = 38°$

FIG. 1. Design velocity triangles.

FIG. 2. Compressor test rig inlet arrangement.
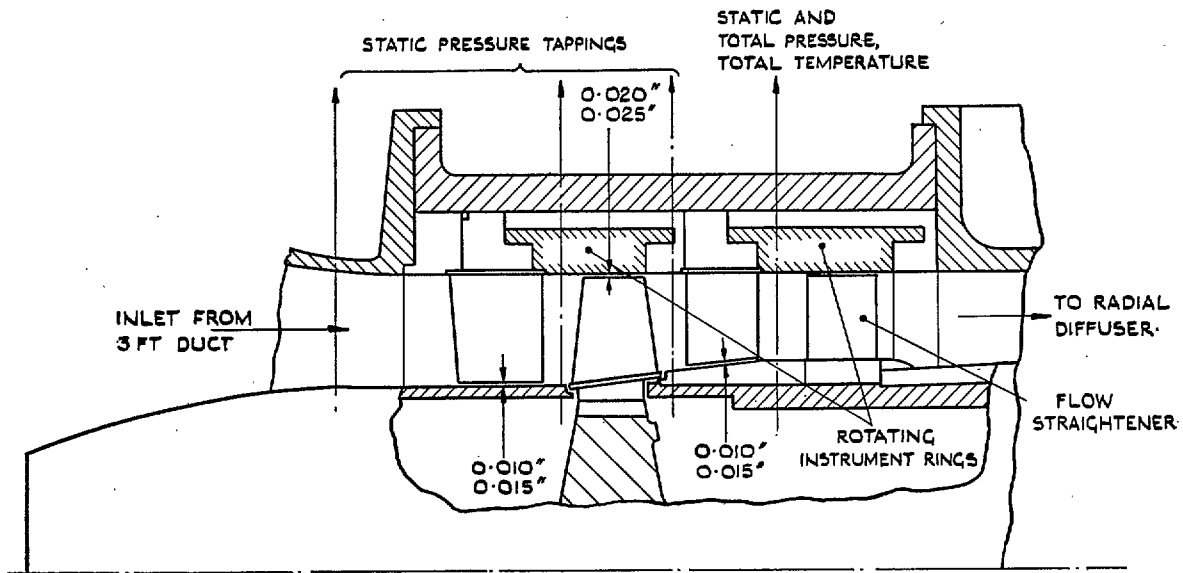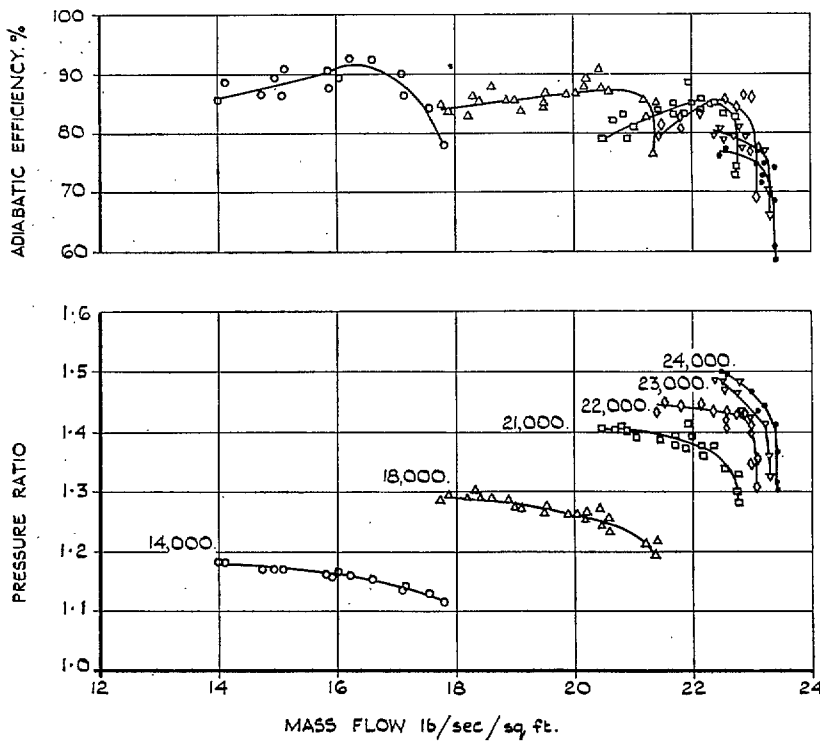
FIG. 3.   Arrangement of compressor stage in the rig.
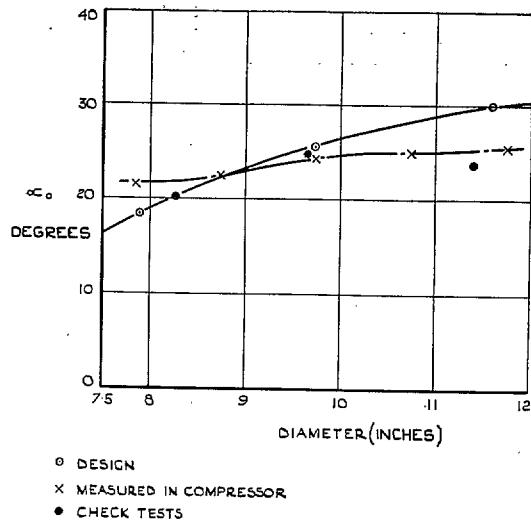

FIG. 4.   Overall characteristics and efficiency.

13

○ DESIGN
× MEASURED IN COMPRESSOR
● CHECK TESTS

FIG. 5.   Inlet guide vane swirl angle distribution.

—— FROM FIG. 4
■ REPEAT TEST AT 21,000 R.P.M.

TRAVERSE DATA

⊕ 14,000 R.P.M.
▲ 18,000 R.P.M.
⊠ 21,000 R.P.M.
◈ 22,000 R.P.M.
▽ 23,000 R.P.M.

DATA REDUCED AS APPENDIX III
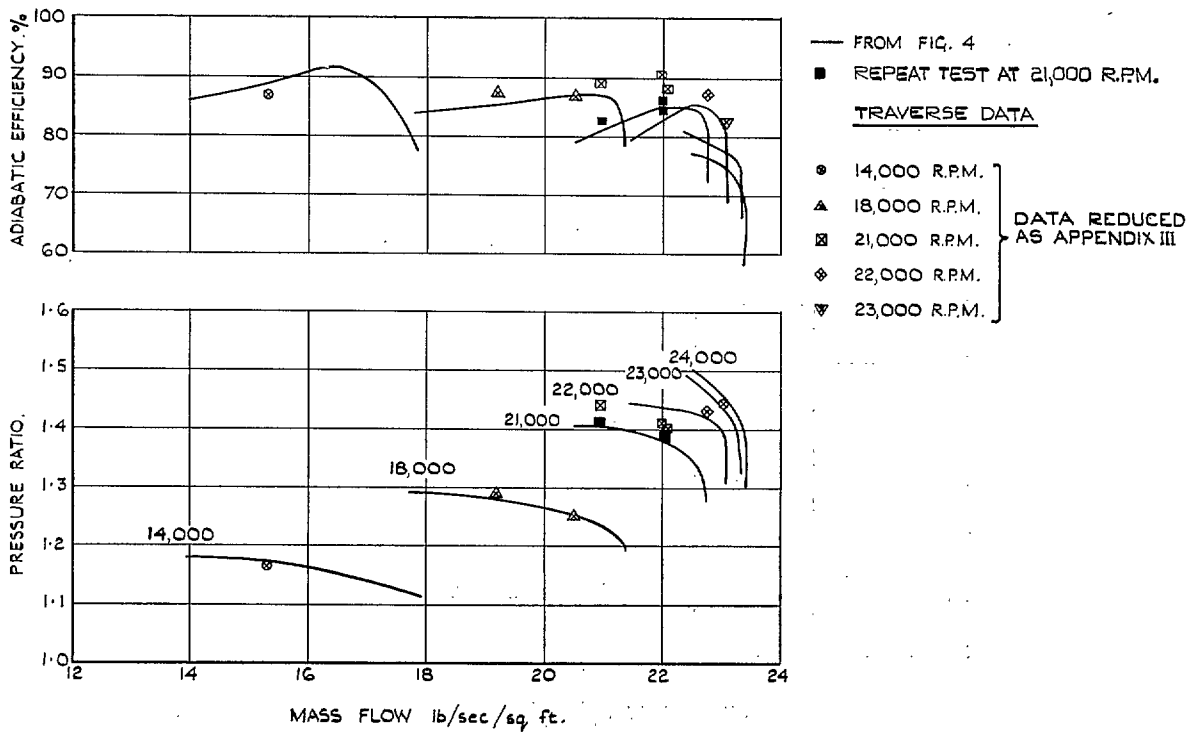
FIG. 6.   Traverse results.

14
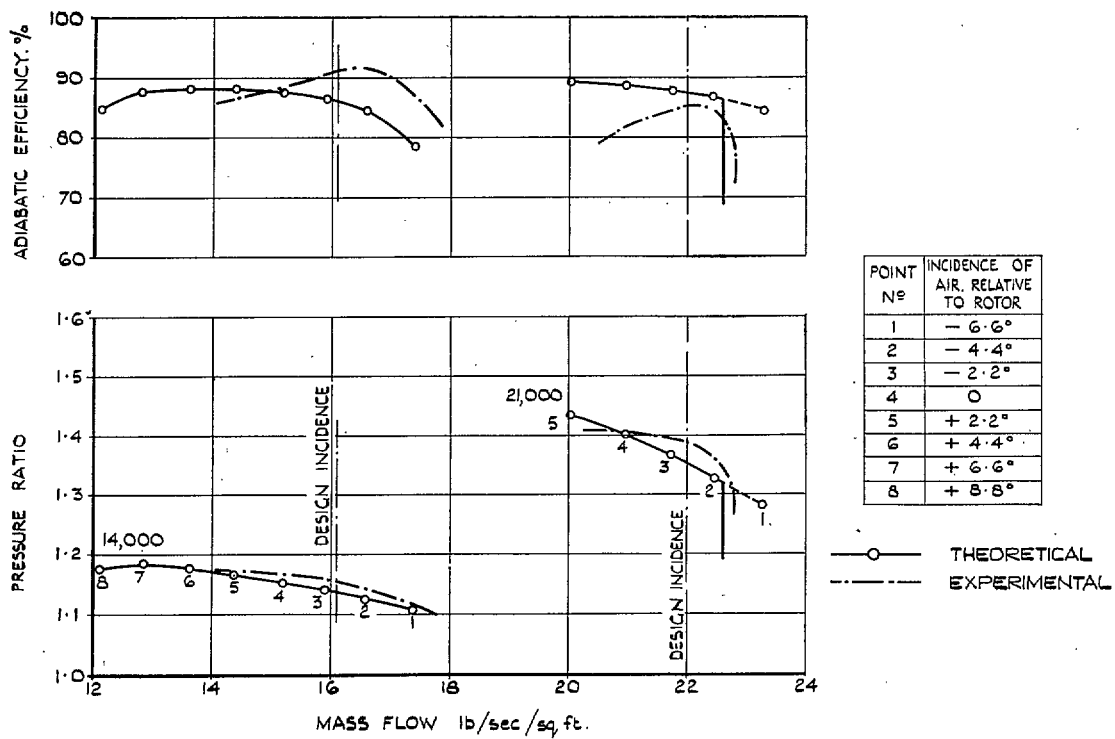
FIG. 7. Comparison between calculated and measured characteristics.

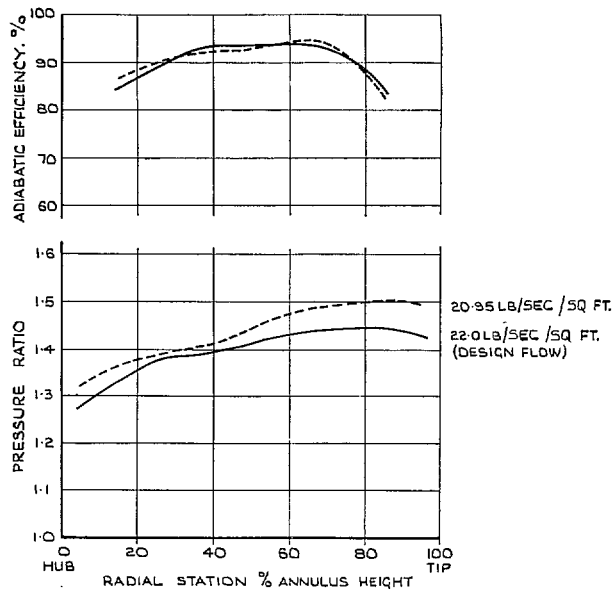| POINT No	INCIDENCE OF AIR, RELATIVE TO ROTOR
1	− 6·6°
2	− 4·4°
3	− 2·2°
4	0
5	+ 2·2°
6	+ 4·4°
7	+ 6·6°
8	+ 8·8°

THEORETICAL

EXPERIMENTAL

FIG. 8. Radial work and efficiency distribution at design speed (21,000 r.p.m.).

15

Publications of the
Aeronautical Research Council

ANNUAL TECHNICAL REPORTS OF THE AERONAUTICAL
RESEARCH COUNCIL (BOUND VOLUMES)

1941 Aero and Hydrodynamics, Aerofoils, Airscrews, Engines, Flutter, Stability and Control, Structures.
63s. (post 2s. 3d.)

1942 Vol. I. Aero and Hydrodynamics, Aerofoils, Airscrews, Engines. 75s. (post 2s. 3d.)
Vol. II. Noise, Parachutes, Stability and Control, Structures, Vibration, Wind Tunnels. 47s. 6d. (post 1s. 9d.)

1943 Vol. I. Aerodynamics, Aerofoils, Airscrews. 80s. (post 2s.)
Vol. II. Engines, Flutter, Materials, Parachutes, Performance, Stability and Control, Structures.
90s. (post 2s. 3d.)

1944 Vol. I. Aero and Hydrodynamics, Aerofoils, Aircraft, Airscrews, Controls. 84s. (post 2s. 6d.)
Vol. II. Flutter and Vibration, Materials, Miscellaneous, Navigation, Parachutes, Performance, Plates and
Panels, Stability, Structures, Test Equipment, Wind Tunnels. 84s. (post 2s. 6d.)

1945 Vol. I. Aero and Hydrodynamics, Aerofoils. 130s. (post 3s.)
Vol. II. Aircraft, Airscrews, Controls. 130s. (post 3s.)
Vol. III. Flutter and Vibration, Instruments, Miscellaneous, Parachutes, Plates and Panels, Propulsion.
130s. (post 2s. 9d.)
Vol. IV. Stability, Structures, Wind Tunnels, Wind Tunnel Technique. 130s. (post 2s. 9d.)

1946 Vol. I. Accidents, Aerodynamics, Aerofoils and Hydrofoils. 168s. (post 3s. 3d.)
Vol. II. Airscrews, Cabin Cooling, Chemical Hazards, Controls, Flames, Flutter, Helicopters, Instruments and
Instrumentation, Interference, Jets, Miscellaneous, Parachutes. 168s. (post 2s. 9d.)
Vol. III. Performance, Propulsion, Seaplanes, Stability, Structures, Wind Tunnels. 168s. (post 3s.)

1947 Vol. I. Aerodynamics, Aerofoils, Aircraft. 168s. (post 3s. 3d.)
Vol. II. Airscrews and Rotors, Controls, Flutter, Materials, Miscellaneous, Parachutes, Propulsion, Seaplanes,
Stability, Structures, Take-off and Landing. 168s. (post 3s. 3d.)

Special Volumes

Vol. I. Aero and Hydrodynamics, Aerofoils, Controls, Flutter, Kites, Parachutes, Performance, Propulsion,
Stability. 126s. (post 2s. 6d.)
Vol. II. Aero and Hydrodynamics, Aerofoils, Airscrews, Controls, Flutter, Materials, Miscellaneous, Parachutes,
Propulsion, Stability, Structures. 147s. (post 2s. 6d.)
Vol. III. Aero and Hydrodynamics, Aerofoils, Airscrews, Controls, Flutter, Kites, Miscellaneous, Parachutes,
Propulsion, Seaplanes, Stability, Structures, Test Equipment. 189s. (post 3s. 3d.)

Reviews of the Aeronautical Research Council

1939–48 3s. (post 5d.)   1949–54 5s. (post 5d.)

Index to all Reports and Memoranda published in the Annual Technical Reports

1909–1947   R. & M. 2600 6s. (post 2d.)

Indexes to the Reports and Memoranda of the Aeronautical Research Council

Between Nos. 2351–2449   R. & M. No. 2450   2s. (post 2d.)
Between Nos. 2451–2549   R. & M. No. 2550   2s. 6d. (post 2d.)
Between Nos. 2551–2649   R. & M. No. 2650   2s. 6d. (post 2d.)
Between Nos. 2651–2749   R. & M. No. 2750   2s. 6d. (post 2d.)
Between Nos. 2751–2849   R. & M. No. 2850   2s. 6d. (post 2d.)
Between Nos. 2851–2949   R. & M. No. 2950   3s. (post 2d.)
Between Nos. 2951–3049   R. & M. No. 3050   3s. 6d. (post 2d.)

HER MAJESTY'S STATIONERY OFFICE
from the addresses overleaf